Saturation-state sensitivity of marine bivalve larvae to ocean acidification

Citation	Waldbusser, G. G., Hales, B., Langdon, C. J., Haley, B. A., Schrader, P., Brunner, E. L., ... & Gimenez, I. (2015). Saturation-state sensitivity of marine bivalve larvae to ocean acidification. Nature Climate Change, 5(3), 273-280. doi:10.1038/NCLIMATE2479
DOI	10.1038/NCLIMATE2479
Publisher	Nature Publishing Group, Macmillan Publishers Ltd.
Version	Accepted Manuscript
Terms of Use	http://cdss.library.oregonstate.edu/sa-termsofuse

Title: Saturation-state sensitivity of marine bivalve larvae to ocean acidification

Short Title: Saturation State Matters to Bivalve Larvae

Author list: George G. Waldbusser[1*], Burke Hales[1], Chris J. Langdon[2], Brian A. Haley[1], Paul Schrader[2], Elizabeth L. Brunner[1], Matthew W. Gray[2], Cale A. Miller[3], Iria Gimenez[1]

1. College of Earth, Ocean, and Atmospheric Sciences, Oregon State University, 104 COAS Admin. Bldg., Corvallis, OR 97331

2. Coastal Oregon Marine Experimental Station and Department of Fisheries and Wildlife, Hatfield Marine Science Center, Oregon State University, 2030 SE Marine Science Dr., Newport OR, 97365

3. Department of Fisheries and Wildlife, Oregon State University, 104 Nash Hall Oregon State University, Corvallis, OR 97331

Corresponding Author: G.G. Waldbusser, College of Earth, Ocean, and Atmospheric Sciences, Oregon State University, 104 COAS Admin. Bldg., Corvallis, OR 97331, 541 737-8964, waldbuss@coas.oregonstate.edu

Keywords: Ocean Acidification, Bivalve Larvae, Carbonate Chemistry, Larval Physiology, Biocalcification

Introductory Paragraph

Ocean acidification results in co-varying inorganic carbon system variables. Of these, an explicit focus on pH and organismal acid-base regulation in has failed to distinguish the mechanism of failure in highly sensitive bivalve larvae. With unique chemical manipulations of seawater we show definitively that larval bivalve shell development and growth are dependent on seawater saturation state, and not on carbon dioxide partial pressure or pH. Although other physiological processes are affected by pH, mineral saturation state thresholds will be crossed decades to centuries ahead of pH thresholds due to the non-linear changes in the carbonate system variables as carbon dioxide is added. Our findings were repeatable for two species of larval bivalves, could resolve discrepancies in experimental results, are consistent with a previous model of ocean acidification impacts due to rapid calcification in bivalve larvae, and suggest a fundamental ocean acidification bottleneck at early life-history for some marine keystone species.

Introduction

Ocean acidification (OA) is described as an imbalance between the acidic influence of rapidly accelerating anthropogenic CO_2 emissions and the slow buffering response due to weathering of continental rock and carbonate marine sediment, causing increased acidity of marine waters (1,2). The release of CO_2 from fossil fuel emissions and cement production, and decreasing uptake efficiency of CO_2 by land and sea has resulted in the fastest increase in P_{CO2} in the last 800,000 years (3). Conversely the natural mechanisms that buffer acidic perturbations from increasing P_{CO2} occur over timescales of hundreds of thousands to millions of years (1,2). Modern anthropogenic changes in the open ocean have tightly coupled aqueous P_{CO2}, pH, and mineral solubility responses, but it was not always thus. Previous instances of elevated P_{CO2} in the geologic record, such as the Cretaceous, appear to coincide with significantly elevated alkalinity (4), and were fairly benign with respect to OA, with elevated P_{CO2} not indicative of low pH or mineral corrosivity. Throughout the geologic record and in many coastal habitats the marine carbonate system decouples resulting in changes in pH, P_{CO2} and saturation state that do not follow the co-variance assumed for modern open-ocean average surface waters (5).

Effects of ocean acidification on a suite of marine organisms have been the subject of significant recent work. While many experimental results have shown equivocal impacts when taken in composite, the process of calcification has mostly exhibited negative sensitivity to OA (6). Physiological processes that may experience OA sensitivity occur across all taxa in nearly all natural waters; however persistent calcified structures can elevate calcium carbonate precipitating species to keystone status in marine waters. Bivalves, which provide a number of critical ecosystem services, have been noted as particularly sensitive to OA (7-10). Some experiments have even found OA impacts at current-day, compared with pre-industrial, P_{CO2}

levels (11). Marine bivalves appear to be sensitive to OA due to 1) the limited degree to which they regulate the ionic balance and pH of their hemolymph (blood) (12-15), and 2) acute sensitivities at specific, short-lived, life-history stages that may result in carryover effects later in life (16-20). Bivalve larvae are particularly sensitive to OA during the hours- to days-long bottleneck when initial shell (called prodissoconch I or PDI) is formed during embryogenesis (17). Prior to PDI shell formation, larvae lack robust feeding and swimming appendages and must rely almost exclusively on maternal energy from eggs; and during calcification of PDI the calcification surfaces are in greater contact with ambient seawater than following shell stages (17). Failure of larvae to complete shell formation prior to exhausting maternal energy reserves leads to eventual mortality, as seen in well-documented oyster hatchery failures (18). To date, the prevailing physiological mechanism identified for OA effects on organisms has been on their ability to regulate internal acid-base status, however, short-term exposure impacts and carryover effects documented in bivalve larvae (18-21) and greater exposure of PDI calcification to ambient seawater (17) points to another mechanism for the early larval sensitivity not captured by regulation of internal acid-base chemistry (22).

In most natural waters the dissolved inorganic carbon (DIC) system controls both pH and the thermodynamic mineral solubility (saturation state), but in different ways. pH is determined by the ratio of dissolved concentrations of CO_2 to carbonate ion, while saturation state is predominantly controlled by absolute carbonate ion concentration. The potential that organisms will respond differently to pH (ratio) or mineral saturation state (abundance), highlights how the decoupling of carbonate system variables in coastal zones (5) or geologic time (1,2) provides a formidable challenge to interpreting and predicting organismal responses to OA. The seemingly simple experimental perturbation of CO_2 bubbling results in the equilibrium redistribution of the

92 acid-base species with pH, saturation state, P_{CO2} and dissolved inorganic carbon (DIC) all
93 changing simultaneously. The co-variance of carbonate parameters leaves interpretation of
94 experimental responses unclear if organismal sensitivity to each parameter is physiologically
95 distinct, particularly if the importance of each process varies across ontology (e.g. respiration,
96 shell formation, feeding rate). The underlying mechanisms of organismal sensitivity to OA may
97 therefore not be constrainable without extraordinary experimental techniques.
98 We conducted series of experiments in which we applied a unique chemical manipulation
99 approach to decouple the carbonate system parameter-covariance and evaluated larval growth
100 and development of two bivalve species: the Pacific oyster, *Crassostrea gigas*, and the
101 Mediterranean mussel, *Mytilus galloprovincialis*. Through simultaneous manipulation of DIC
102 and alkalinity, we generated a 4x4 factorial design with aragonite saturation state (Ω_{ar}) and P_{CO2}.
103 Our experimental design separated Ω_{ar} and P_{CO2} effects on larval responses; and responses to pH
104 were evaluated by examining responses to pH within a P_{CO2} and Ω_{ar} treatment level. Using this
105 approach, we assessed which carbonate system parameter is most important to early larval shell
106 development and growth: pH, P_{CO2}, or Ω_{ar}.
107
108 **Results:**
109 We successfully decoupled pH, P_{CO2}, and Ω_{ar} experimentally to find saturation state (Ω_{ar})
110 as the primary variable affecting early larval shell development and growth in these two bivalve
111 species. Below we describe why this direct sensitivity to Ω_{ar} demands a refinement of our current
112 model of OA responses of calcifying organisms, and the environmental relevance of these
113 results.
114 *Chemistry manipulations*

We simultaneously altered abundance and ratio of DIC and alkalinity to provide three orthogonal experimental axes in pH, P_{CO2}, and saturation state of the calcium carbonate mineral aragonite (Ω_{ar}) (Figure 1, Supplementary Table 1). The sensitivity of these parameters to DIC:Alkalinity means that there is some variability within treatment suites, but that variability was far less than the differences among treatments. We were able to replicate treatment conditions via DIC and alkalinity as evidenced by the concordance between expected versus measured values (Supplementary Figure 1). At the termination of the 48 hour incubation period we found P_{CO2} generally increased ~10-30% relative to initial conditions. The greatest P_{CO2} increases were in treatments with the poorest larval development, likely due to elevated microbial respiration associated with larval mortality in these treatments.

Prodissoconch I shell development

The dominant effect of Ω_{ar} on proportion normal shell development (PNS) is immediately apparent in Figure 2. The Ω_{ar} effect is clear for both species, with highly significant effects (Mussels $F_{3,15} = 105.53$, $p < 0.0001$, Oysters $F_{3,15} = 76.79$, $p < 0.0001$, Supplementary Table 2); Ω_{ar} explained 88 and 86% of the variance in proportion normal for the mussels and oysters, respectively. P_{CO2} and the Ω_{ar} by P_{CO2} interaction were not significant (Supplementary Table 2). Experiment # was found to be statistically significant, but only explained 3 and 6% of the variance for the mussels and oysters, respectively (Supplementary Table 2). We fit a three parameter logistic equation to the untransformed treatment means of PNS (Figure 2) to determine the functional response of both species to saturation state. The fit was found to be highly significant for mussel ($F_{2,29} = 223.01$, $R^2 = 0.93$, $p < 0.0001$) and oyster larvae ($F_{2,29} = 72.61$, $R^2 = 0.83$, $p < 0.0001$).

Our results unequivocally show that saturation state is the primary carbonate system variable of importance for normal shell development for these two bivalve species; we will, however, further explore possible pH effects in our experiments, given its importance to physiological acidosis and the historical emphasis on pH in OA experiments. Since pH covaries with the primary factors in the ANOVA, and a slight visual pattern is apparent (Figure 2) we ran a series of regression analyses of PNS versus pH, within a saturation state treatment. Although we found some statistically significant slopes generally in the low Ω_{ar} treatments (Supplementary Table 3), the effect is equivocal and its magnitude dramatically smaller than the Ω_{ar} effect. The largest effect we found was in the lowest saturation state treatment for oysters, with a 0.1 increase in PNS per 0.1 pH units from pH 7.27 to 7.51. Other significant slopes were less than half of this 0.02 to 0.04 PNS per 0.1 pH unit within a Ω_{ar} treatment. The pH effect across the entire experimental range seen in Figure 2 is, therefore, primarily an artifact of pH covariance with Ω_{ar}. Additionally, at pH values of < 7.6 and < 7.4 in the mussel and oyster experiments respectively, we still see excellent PNS of > 80% if Ω_{ar} is high. We therefore reiterate that Ω_{ar} is the primary carbonate system variable driving successful shell development of early larvae in these two species.

Shell Growth

Even among larvae that appeared to develop normal shell morphology, Ω_{ar} was still the primary factor influencing growth (Figure 3, Supplementary Table 4). Ω_{ar} had statistically significant effects on the mussels ($F_{2,24} = 707.63$, $p < 0.0001$) and oysters ($F_{3,9} = 219.29$, $p < 0.0001$), explaining 93 and 81% of the variance in normal shell length for each species. The lack of normally-developed mussel larvae in the low Ω_{ar} treatments prevented size estimates. Shell

length decreased by nearly 25% and 10% with decreasing Ω_{ar} across our experimental range, in the mussel and oyster larvae, respectively. P_{CO2} had minor significant positive effects on mussel ($F_{3,24} = 5.83$, $p = 0.0039$) and oyster larvae shell length ($F_{3,32} = 27.64$, $p < 0.0001$), (Figure 3, Supplementary Table 4), explaining 1% and 10% of the variance in shell length. The interaction between Ω_{ar} and P_{CO2} was also statistically significant for both species, but only explaining 5% of the shell growth variance for both species (Supplemental Table 4, Supplemental Figure 2). The positive response to P_{CO2} may seem counter-intuitive at first; however, within an Ω_{ar} treatment level, DIC concentrations are proportional to P_{CO2} (Supplementary Table 1), and inversely proportional to pH. We did not evaluate pH effects on shell growth given what appears to be a positive response to decreasing pH, and thus a likely response to increasing DIC concentrations (Figure 3). We will argue below that shell growth is responding to DIC within an Ω_{ar} treatment level, but again, saturation state is the dominant parameter affecting shell growth of these early larvae. Shell length continues to increase with increasing saturation state even at the highest values in our treatments, $\Omega_{ar} \sim 4$ and $\Omega_{ar} \sim 6.5$ for the mussel and oyster larvae, respectively. We therefore fitted a power function to the response of shell length to saturation state (Figure 3). The fit of the model for both species was highly significant: mussel larvae ($F_{2,10} = 81.36$, $R^2 = 0.89$, $p < 0.0001$) and oyster larvae ($F_{2,14} = 103.22$, $R^2 = 0.88$, $p < 0.0001$).

Why Saturation State Matters to Bivalve Larvae

Our results initially appear contradictory to the physiological basis for understanding ocean acidification impacts on organisms; particularly the overarching role of seawater pH, acid-base regulation, and extracellular acidosis in marine organisms (12,13, 22-24). Specifically we found that seawater pH appears to have little to no measureable effect on early larval shell

development and growth, except for the case where pH and Ω_{ar} are both very low (Figures 2&3). At these low levels, seawater pH likely becomes very important (particularly to bivalves which show limited ability to regulate extracellular pH), as eukaryote intracellular pH typically ranges from 7.0-7.4 (25) and additional energy is needed to maintain physiochemical gradients crucial for passive and active cross-membrane ion transport (26) if extracellular pH approaches these values. Some species appear to be able to mitigate acidosis via bicarbonate accumulation; however ability to do so is variable across taxa, and bicarbonate accumulation often requires several days to months (14, 15, 22). During the transient (days) early larval stage it is unlikely that bivalve larvae have the time or physiological capacity to compensate for acidosis (22), with their limited energy budget and the embryological development underway at this time period. Therefore, while seawater pH effects on organismal acidosis may also be at work during in this early larval stage, we have experimentally shown that any pH effect is overwhelmed by the impact of saturation state during initial shell formation. The likelihood of organisms experiencing such low pH conditions without coinciding low-Ω conditions is also very unlikely (Figure 1, Supplementary Table 1). Therefore, the conclusions from this study do not contradict the importance of pH on marine bivalve larvae, but rather highlight the overwhelming significance of saturation state at this critical bottleneck for bivalve larvae.

We have previously argued (17) that during PDI shell formation in bivalve larvae the rapid rate of calcification (as in Figure 4) and increased exposure of crystal nucleation sites to seawater puts an important kinetic-energetic constraint on the larvae; thereby mandating a Ω_{ar} sensitivity. The classical representation of the calcification rate (r) following the standard empirical formulation is:

1) $r = k(\Omega - 1)$.

The apparently predetermined amount of rapid calcification required to form the PDI shell and begin feeding requires the biocalcification rate constant (*k*) to be several orders of magnitude higher than inorganic precipitation (17). This constraint also demands a rapidly accelerating biocalcification rate constant (*k*) as Ω approaches saturation (and thus Ω-1 approaches 0) to maintain the calcification rate necessary to complete the PDI shell without depleting maternal energy reserves. The logical extension of this argument that biocalcification is not possible below saturation is erroneous however. Bivalve larvae clearly precipitate mineral when ambient conditions are undersaturated and must, therefore, create some level of supersaturation at crystal nucleation sites which are semi-exposed to the external environment. We suggest that larvae are both elevating Ω at the site of calcification and elevating *k* through physical-chemical changes at the organic-inorganic nucleation interface (17). That is, the dependency on seawater Ω_{ar} in our experimental results (Figure 2) supports the importance of this kinetic-energetic constraint; increasing seawater super-saturation lowers the energetic cost of shell building increasing the scope for growth, as seen in the shell length response to Ω_{ar} (Figure 3).

A curious pattern is observed in our shell length data. Figure 3 appears to indicate a minor (positive/negative) effect of P_{CO2}/pH on shell growth. Within a Ω_{ar} treatment group, our experimental manipulations result in decreasing DIC with increasing pH (Supplementary Table 1). Previous studies in corals have suggested that total DIC (driven mostly by bicarbonate ion) is an important factor for calcification (27-29). Alternatively, the ratio of DIC/$[H^+]$ (which is in fact a proxy for carbonate ion and thus saturation state) due to the proton flux model (30) may be the

controlling parameter for coral calcification. Given the differences in calcification mechanisms and shell morphology between larval prodissoconch I (PDI) and prodissoconch II (PDII) (31), we postulate that any minor, secondary DIC effect may be acting during the latter PDII shell formation. In fact, Timmins-Schiffman et al. (32) found that larval *C. gigas* shell size was not affected by elevated CO_2 at day one (PDI), but by three days post fertilization shells were significantly smaller in the high CO_2 treatment (PDII). Larvae from our two day experiments had already begun PDII shell formation, and therefore, it seems plausible the impacts of Ω_{ar} (negative) and DIC (slightly positive) on shell length were acting on PDII. Conversely, the range of Ω_{ar} tested by the Timmins-Schiffman et al. (32) was roughly between 1-2 (P_{CO2} ~400- 1100 μatm), and may have resulted in undetectable PDI size differences over the smaller experimental range (highlighting the value of experimental treatments extending beyond open ocean projections). The minor secondary positive effect of DIC (at super-saturation) appears consistent with previous studies. However saturation state was still the dominant factor impacting shell length of normally developed larvae. While we cannot determine whether compensatory growth is possible if saturation state is improved later in larval life, the carry-over effects found on US west coast oyster larvae indicate there is limited capacity to recover from OA exposure during sensitive early larval stages (18-20).

Even the most critical of OA meta-analyses on organismal responses (6) note calcification as being the "most sensitive" of responses to ocean acidification. For developing embryos of bivalve larvae, calcification is a process that determines whether larvae will survive or perish; without the development and calcification of the PDI shell, larvae likely lack a functional velum to support swimming and feeding due to lack of muscular-skeletal attachment. Without an effective feeding mechanism larvae will eventually exhaust endogenous energy

253 reserves (17). Although larvae may be able to support basal metabolism using dissolved organic
254 matter (DOM) (33), the velum is also responsible for DOM uptake (34). Our results show that
255 seawater Ω_{ar} is directly affecting shell development and growth, and this effect is not an indirect
256 pH impact on internal acid-base status. Without shell development, or if it is too energetically
257 expensive, there appears little opportunity for larvae to overcome OA during this early stage
258 (17). A previous study (35) suggested carbonate ion concentration, not saturation state matters to
259 larvae. Calcium addition was used to manipulate mineral solubility without a control for excess
260 calcium at already super saturated mineral solubility (35). The addition of roughly 2x calcium, as
261 in (35), at Ω_{ar} ~ 2.0 (increasing Ω_{ar} to ~ 3.64) resulted in very poor shell development (PNS =
262 0.39 ± 0.8) and much smaller normal larvae (S.L. = 68.63 ± 3.22 μm) in *C. gigas*. This result is
263 not surprising given calcium's role in cellular ion transport, immune response, and the lack of
264 osmo-regulation in marine bivalves (14, 36). This is a minor point ultimately, since carbonate ion
265 concentration usually controls saturation state in marine waters. Importantly however, the
266 carbonate in marine bivalve shell is derived from all forms of DIC, including respiratory carbon
267 (17 and references therein), increased seawater saturation state appears to make the kinetics of
268 shell formation less energetically expensive.
269
270 **Environmental Context**
271 In marine waters, the increase of P_{CO2} decreases saturation state and pH, but their
272 declines approach potential thresholds differentially. We have plotted the change in Ω_{ar} and pH
273 as P_{CO2} increases at typical upwelling conditions in Oregon's coastal waters (Figure 5). We
274 found acute responses of bivalve larvae begin to manifest at saturation states (Ω_{ar}) of ~1.2- 1.5
275 (Figures 2, 3). Other studies have documented sub-lethal chronic exposure effects in Pacific

oyster larvae (~2.0: (18, 35,)), Olympia oyster larvae (~1.4, (19)), Eastern oyster larvae (~1.9, (11)), and California mussel larvae (~1.8, (37)). While far from an exhaustive list of experimental studies, placing these Ω_{ar} values in context of the current conditions in the California Current ecosystem illustrate two key points. First, there is limited remaining capacity for Oregon's coastal waters to absorb more CO_2 before sub-lethal Ω_{ar} thresholds are crossed for bivalve larvae. Increasing atmospheric CO_2 pushes saturation state across these larval bivalve thresholds more frequently and with greater magnitude in the California Current (38,39). Second, these saturation state thresholds will be crossed long before recently documented pH changes found to physiological important in mollusks (8) (often > 0.3 pH units). If transient conditions during spawning are unfavorable for bivalve larvae, in hatcheries or in the wild, then these impacts would result in diminished larval supply and recruitment to adult populations.

Larval supply and recruitment are vital to maintaining many benthic marine invertebrate populations (40). Survival to metamorphosis requires normal development and rapid growth to limit larval predation (40). Larger larval size indicates greater scope for growth and replete energy stores needed to complete metamorphosis (41); energy stores that are diminished under acidification stress (11). Recruitment to adult populations can be highly variable year to year and often related to regional climatology (42, 43). The coastal zones where many ecologically and economically important marine calcifiers are found will not experience acidification gradually as seen in the oligotrophic open ocean, but rather as increases in frequency, duration, and magnitude of events that are unfavorable for specific life-history stages (5, 38, 44). Our experimental work has shown that successful larval development and growth during rapid shell formation is dependent on seawater saturation state in temporal windows lasting 2 days or less (Figure 4); thus providing increasing evidence for a mechanism by which transient, moderate

acidification impacts (18) nearly resulted in collapse of the Pacific Northwest oyster industry (45). These impacts occur on time scales relevant to changes already observed in coastal zones (5, 18, 46), regardless of future changes or direct cause, and thus decreases in saturation state can limit recruitment to current bivalve populations. Our experimental approach and findings shed new insight into organismal responses to OA, while indicating the importance of monitoring the complete carbonate chemistry system, to be able to successfully link biological and chemical observations.

Methods (see SI for extended methods):

Water collection and stripping dissolved inorganic carbon

For each experiment, 1 µm filtered seawater was collected from Yaquina Bay, Oregon. The alkalinity was reduced by addition of trace metal grade HCl in near alkalinity equivalence, followed by bubbling with ambient air for 48 hours to strip (DIC) as CO_2. The acidified, stripped seawater was then 0.22 µm filtered, pasteurized, and stored at 2-5 °C. Prior to treatment manipulation, the seawater was bubbled with 0.2 µm-filtered outside air until atmospheric conditions were achieved, then carbonate DIC and alkalinity values were determined for manipulations.

Experimental manipulation

A 4x4 factorial experimental design was developed to target 16 total treatment combinations of P_{CO2} and Ω_{ar} (saturation state with respect to aragonite) (Supplementary Table 1, Figure 1), with triplicate 500 ml biological oxygen demand (BOD) bottles per treatment. Two separate experiments were conducted with each species. DIC and alkalinity concentrations were

calculated for each of the 16 target treatment combinations (P_{CO2} and Ω_{ar}). Experimental treatments were created by gravimetric addition of mineral acids and bases to the decarbonated seawater in gas-impermeable bags customized with luer lock fittings. Aliquots of a concentrated, ambient-P_{CO2}, solution of Na_2CO_3 and and $NaHCO_3$ were added to adjust DIC to target treatment level followed by 0.1N HCl to adjust alkalinity. Immediately following chemical manipulation, the bags with treatment water were stored without head-space at 2-5 °C for up to several weeks before spawning broodstock. Antibiotics were added to BOD bottles (2 ppm chloramphenicol and 10 ppm ampicillin), which we found to have no negative effects on larvae or carbonate chemistry in prior trials. Controls were included to evaluate experimental manipulations and incubation conditions by hatching eggs in open culture containers, as well as by using stored seawater collected prior to decarbonation and not subjected to chemical manipulations described in this study.

Carbonate chemistry measurements

Carbonate chemistry samples were collected from the treatment water bags just prior to stocking larvae in BOD bottles, and also from each BOD bottle at the end of the incubation period. Carbonate chemistry samples were collected in 350 ml amber glass bottles with polyurethane-lined crimp-sealed metal caps and preserved by addition of 30 µl of saturated $HgCl_2$. Analyses of P_{CO2} and DIC were carried out following the procedure of Bandstra et al. (47) modified for discrete samples as in Hales et al. (48). Gas and liquid standards that bracketed the experimental range (Supplementary Table 1) were employed to ensure accuracy.

Larval Rearing

Broodstock for mussel (*Mytilus galloprovincialis*) and oyster (*Crassostrea gigas*) experiments were obtained from Carlsbad Aquafarm, Carlsbad, CA, or from selected stocks of the Molluscan Broodstock Program (MBP) (49), Yaquina Bay, Oregon, respectively. Broodstock spawning was stimulated by rapid increase of 10 ^{o}C in ambient seawater temperature. Gametes were collected from at least two male and two female parents, and the eggs fertilized in ambient seawater. Developing embryos were added at a density of 10 larvae ml^{-1} to triplicate BOD bottles per treatment after visual verification of successful fertilization. Sealed BOD bottles were oriented on their side and incubated for 48 hours at culture temperature (18 ^{o}C for mussels and 22 ^{o}C and 25 ^{o}C for oyster trials 1 and 2, respectively). Larvae from each BOD bottle were concentrated after a filtered chemistry sample was collected, sampled in triplicate, and preserved in 10% formalin buffered to ~8.1-8.2.

Larval shell development and size

Larvae were examined microscopically to determine the proportion of normally and abnormally developed D-hinge (prodissoconch I) larvae as well as larval shell lengths. Normally developed larvae were characterized by a straight hinge, smooth curvature along the edge of the valve, and appearance of tissue within the translucent shells (50). Digital images were used to determined shell length (longest axis perpendicular to the hinge) of normally developed larvae only. Images were analyzed using ImageJ (V1.42).

Data analyses

Proportion normal data were scaled to the un-manipulated, seawater control for each experiment by dividing treatment values by control values. We used a two-way analysis of

368 variance (ANOVA), with P_{CO2} and Ω_{ar} as the primary factors with experiment as a blocking
369 factor. Proportion normal data were square-root arcsine transformed. Assumptions of normality
370 and homoscedascity were checked and any violations were managed as noted. Initial data
371 analyses found unequal variance across treatment groups in the transformed proportion normal
372 data, and mean values per treatment were used to improve heteroscedascity as well as blocking
373 by experiment. To evaluate pH effects on shell development we ran a series of regression
374 analyses of transformed proportion normal regressed on pH, within each Ω_{ar} treatment and
375 experiment. We then used a Bonferroni correction for multiple tests of significance to reduce
376 Type 1 error. Analyses were conducted with the SAS software suite (v9.3). Non-linear, least-
377 squares regression in Sigma-Plot (v12.5) was used to fit functional responses of development
378 (logistic) and shell length (power).
379

Correspondence and inquiries regarding this study should be addressed to G.G. Waldbusser.

Acknowledgements

This work was supported by the National Science Foundation OCE CRI-OA #1041267 to GGW, BH, CJL, and BAH. The authors would like to thank H. Bergschneider, R. Mabardy, J. Sun, G. Hutchinson, and T. Klein for their dedicated efforts on the experimental work, S. Smith for sampling and imaging developing embryos, and J. Jennings for assistance and student training on carbonate analyses. GGW would like to specifically thank T. Sawyer in the OSU electron microscope laboratory for guidance on imaging bivalve embryos. Comments from A. Hettinger, S.E. Kolesar, and three anonymous reviewers improved an earlier version of this manuscript.

Author Contributions

GGW, BH, CJL, and BAH conceived and planned the research. GGW designed and supervised experiments. GGW and BH analyzed data. PS organized study components and PS, MWG, ELB, IG, CAM developed and carried out experiments. MWG, ELB, IG, CAM analyzed organism and chemistry samples. All authors contributed to writing the manuscript.

References

1. Archer D, Kheshgi H & Maier-Reimer E (1997) Multiple timescales for neutralization of fossil fuel CO_2. *Geophys Res Lett* **24**(4)**:** 405-408.
2. Hönisch B et al. (2012) The Geological Record of Ocean Acidification. *Science* **335**(6072)**:** 1058-1063.
3. Luethi D, et al. (2008) High-resolution carbon dioxide concentration record 650,000-800,000 years before present. *Nature* **453**(7193)**:** 379-382.
4. Zeebe RE (2001) Seawater pH and isotopic paleotemperatures of Cretaceous oceans. *Palaeogeogr Palaeoclimatol Palaeoecol* **170**(1-2)**:** 49-57.
5. Waldbusser GG & Salisbury JE (2014) in *Annual Review of Marine Science, Vol 6*, Vol. 6, pp. 221-247.
6. Hendriks IE, Duarte CM & Alvarez M (2010) Vulnerability of marine biodiversity to ocean acidification: A meta-analysis. *Estuar Coast Shelf Sci* **86**(2)**:** 157-164.
7. Parker LM et al. (2013) Predicting the Response of Molluscs to the Impact of Ocean Acidification. *Biology* **2**: 651–692.
8. Gazeau F et al. (2013) Impacts of ocean acidification on marine shelled molluscs. *Mar Biol* **160**: 2207–2245.
9. Wittmann AC & Poertner HO (2013) Sensitivities of extant animal taxa to ocean acidification. *Nature Climate Change* **3**(11)**:** 995-1001.
10. Kroeker KJ, et al. (2013) Impacts of ocean acidification on marine organisms: quantifying sensitivities and interaction with warming. *Glob Change Biol* **19**(6)**:** 1884-1896.
11. Talmage SC & Gobler CJ (2010) Effects of past, present, and future ocean carbon dioxide concentrations on the growth and survival of larval shellfish. *Proceedings of the National Academy of Sciences*. **107**(40): 17246-17251.
12. Thomsen J, et al. (2010) Calcifying invertebrates succeed in a naturally CO2-rich coastal habitat but are threatened by high levels of future acidification. *Biogeosciences* **7**(11)**:** 3879-3891.
13. Melzner F, et al. (2011) Food Supply and Seawater pCO(2) Impact Calcification and Internal Shell Dissolution in the Blue Mussel *Mytilus edulis*. *PLoS One* **6**(9).
14. Shumway SE (1977) Effect of salinity fluctuation on the osmotic pressure and Na^{+}, Ca^{2+}, and Mg^{2+} ion concentrations in the hemolymph of bivalve molluscs. *Mar Biol* **41**(2)**:** 153-177.
15. Heinemann A, et al. (2012) Conditions of *Mytilus edulis* extracellular body fluids and shell composition in a pH-treatment experiment: Acid-base status, trace elements and delta B-11. *Geochemistry Geophysics Geosystems* **13**: DOI: 10.1029/2011GC0037
16. Waldbusser GG, Bergschneider H, Green MA (2010) Size-dependent pH effect on calcification in post-larval hard clam Mercenaria spp. *Mar Ecol-Prog Ser* **417**:171–182.
17. Waldbusser GG, et al. (2013) A developmental and energetic basis linking larval oyster shell formation to acidification sensitivity. *Geophys Res Lett* **40**(10)**:** 2171-2176.
18. Barton A, Hales B, Waldbusser GG, Langdon C, Feely RA (2012) The Pacific oyster, *Crassostrea gigas*, shows negative correlation to naturally elevated carbon dioxide levels: Implications for near-term ocean acidification effects. *Limnol Oceanogr* **57**:698–710.
19. Hettinger A et al. (2012) Persistent carry-over effects of planktonic exposure to ocean acidification in the Olympia oyster. *Ecology* **93**:2758–2768.
20. Hettinger A, et al. (2013) Larval carry-over effects from ocean acidification persist in the

natural environment. *Glob Change Biol* **19**(11)**:** 3317-3326.
21 Gobler CJ & Talmage SC (2013) Short and long term consequences of larval stage exposure to constantly and ephemerally elevated carbon dioxide for marine bivalve populations. *Biogeosciences* **10**: 2241-2253
22. Melzner F, et al. (2009) Physiological basis for high CO_2 tolerance in marine ectothermic animals: pre-adaptation through lifestyle and ontogeny? *Biogeosciences* **6**(10)**:** 2313-2331.
23. Michaelidis B, Ouzounis C, Paleras A. & Pörtner HO (2005) Effects of long-term moderate hypercapnia on acid-base balance and growth rate in marine mussels *Mytilus galloprovincialis*. *Mar Ecol-Prog Ser* **293**: 109-118.
24. Pörtner HO (2008) Ecosystem effects of ocean acidification in times of ocean warming: a physiologist's view. *Mar Ecol-Prog Ser* **373**: 203-217.
25. Madshus IH (1988) Regulation of Intracellular Ph in Eukaryotic Cells. *Biochem J* **250**(1)**:** 1-8.
26. Walsh PJ & Milligan CL (1989) Coordination of Metabolism and Intracellular Acid-Base Status - Ionic Regulation and Metabolic Consequences. *Can J Zool-Rev Can Zool* **67**(12)**:** 2994-3004.
27. Jury CP, Whitehead RF & Szmant AM (2010) Effects of variations in carbonate chemistry on the calcification rates of *Madracis auretenra* (= *Madracis mirabilis* sensu Wells, 1973): bicarbonate concentrations best predict calcification rates. *Glob Change Biol* **16**(5)**:** 1632-1644.
28. Ries JB (2011) A physicochemical framework for interpreting the biological calcification response to CO2-induced ocean acidification. *Geochim Cosmochim Acta* **75**(14)**:** 4053-4064.
29. Comeau S, Carpenter RC & Edmunds PJ (2013) Coral reef calcifiers buffer their response to ocean acidification using both bicarbonate and carbonate. *Proc R Soc Biol Sci Ser B* **280**(1753)**:** 1-8.
30. Jokiel PL (2013) Coral reef calcification: carbonate, bicarbonate and proton flux under conditions of increasing ocean acidification. *Proc R Soc Biol Sci Ser B* **280**(1764)**:** 1-4.
31. Kniprath E (1981) Ontogeny of the Molluscan Shell Field - a Review. *Zool Scr* **10**(1)**:** 61-79.
32. Timmins-Schiffman E, O'Donnell MJ, Friedman CS & Roberts SB (2013) Elevated pCO(2) causes developmental delay in early larval Pacific oysters, *Crassostrea gigas*. *Mar Biol* **160**(8)**:** 1973-1982.
33. Moran AL & Manahan DT (2004) Physiological recovery from prolonged 'starvation' in larvae of the Pacific oyster *Crassostrea gigas*. *J Exp Mar Biol Ecol* **306**(1)**:** 17-36.
34. Manahan DT & Crisp DJ (1983) Autoradiographic Studies on the Uptake of Dissolved Amino-Acids from Sea-Water by Bivalve Larvae. *J Mar Biol Assoc U K* **63**(3)**:** 673-682.
35. Gazeau F, et al. (2011) Effect of Carbonate Chemistry Alteration on the Early Embryonic Development of the Pacific Oyster (*Crassostrea gigas*). *PLoS One* **6**(8)**:** e23010, 1-8.
36. Bibby R, Widdicombe S, Parry H, Spicer J & Pipe R (2008) Effects of ocean acidification on the immune response of the blue mussel Mytilus edulis. *Aquat Biol* **2**(1)**:** 67-74.
37. Gaylord B, et al. (2011) Functional impacts of ocean acidification in an ecologically critical foundation species. *J Exp Biol* **214**(15)**:** 2586-2594

38. Hauri C, Gruber N, McDonnell AMP & Vogt M (2013) The intensity, duration, and severity of low aragonite saturation state events on the California continental shelf. *Geophys Res Lett* **40**(13)**:** 3424-3428.
39. Harris KE, DeGrandpre MD & Hales B (2013) Aragonite saturation state dynamics in a coastal upwelling zone. *Geophys Res Lett* **40**(11)**:** 2720-2725.
40. Rumrill SS (1990) Natural Mortality of Marine Invertebrate Larvae. *Ophelia* **32**(1-2)**:** 163-198.
41. Ben Kheder R, Quere C, Moal J & Robert R (2010) Effect of nutrition on *Crassostrea gigas* larval development and the evolution of physiological indices Part B: Effects of temporary food deprivation. *Aquaculture* **308**(3-4)**:** 174-182.
42. Kimmel DG & Newell RIE (2007) The influence of climate variation on eastern oyster (*Crassostrea virginica*) juvenile abundance in Chesapeake Bay. *Limnol Oceanogr* **52**(3)**:** 959-965.
43. Dumbauld BR, Kauffman BE, Trimble AC & Ruesink JL (2011) The Willapa Bay Oyster Reserves in Washington State: Fishery Collapse, Creating a Sustainable Replacement, and the Potential for Habitat Conservation and Restoration. *J Shellfish Res* **30**(1)**:** 71-83.
44. Gruber N, et al. (2012) Rapid Progression of Ocean Acidification in the California Current System. *Science* **337**(6091)**:** 220-223.
45. Feely RA, Klinger T, Newton JA, & Chadsey M (2012): Scientific Summary of Ocean Acidification in Washington State Marine Waters. NOAA OAR Special Report #3934.
46. White MM, McCorkle DC, Mullineaux LS, Cohen AL (2013) Early Exposure of Bay Scallops (*Argopecten irradians*) to High CO_2 Causes a Decrease in Larval Shell Growth. *PLoS ONE* **8**(4): e61065. doi:10.1371/journal.pone.0061065
47. Bandstra L, Hales B & Takahashi T (2006) High-frequency measurements of total CO2: Method development and first oceanographic observations. *Mar Chem* **100**(1-2)**:** 24-38.
48. Hales B, Takahashi T & Bandstra L (2005) Atmospheric CO2 uptake by a coastal upwelling system. *Global Biogeochem Cycles* **19**(1).
49. Langdon CJ, Evans F, Jacobson D and Blouin, M (2003) Yields of cultured Pacific oysters *Crassostrea gigas* Thunberg improved after one generation of selection. *Aquaculture*, **220**:227-244.
50. American Society for Testing and Materials (2004) Standard guide for conducting static acute toxicity tests starting with embryos of four species of saltwater bivalve molluscs. E724-98. 22 pp.

Figure Legends

Figure 1. Carbonate chemistry values for the 16 experimental treatments for each of the four experiments grouped by species, plotted against P_{CO2} and saturation state, with isopleths of pH plotted in P_{CO2}/saturation state space. The left panel includes values for the two experiments on *Mytilus galloprovincialis* (a) and the right panel for the two experiments on *Crassostrea gigas* (b). Circle and square symbols represent chemistry for the 1st and 2nd experiments, respectively.

Figure 2. Mean proportion normally developed D-hinge larvae for mussel (left column) and oyster (right column) experiments in response to P_{CO2} (a, b), pH (c, d), and saturation state (e, f). Circles and squares are the first and second experiment, respectively. Fills from black to white are increasing saturation state. Symbols are the mean values of the three replicate containers, each of which was sub-sampled three times (approximately 100-200 larvae per sub-sample). Error bars are standard deviations of mean replicate values per treatment. Error bars were excluded from pH plot to allow easier visual interpretation.

Figure 3. Mean shell length of normally developed larvae in response to P_{CO2} (a, b), pH (c, d), and saturation state (e, f). The grey scale symbols are the same as previous. Means and standard deviations are of replicate containers per treatment, as above. We lack larvae from low omega treatments due to very poor development in the mussel experiments. The total number of normal larvae measured for shell length was 3132 and 7106 for the mussel and oyster experiments, respectively. Control shell lengths were 108.44 ± 2.57 μm and 78.78 ± 2.06 μm for the mussels and oysters, respectively.

Figure 4. Representative scanning electron micrographs of Pacific oyster larvae at (a) 10 hrs., (b) 14hrs., and (c) 16 hrs. post fertilization. Over the course of development from panel a to panel c the formation of the periostracum (wrinkled) is seen, followed by increasing amounts of hardening by calcium carbonate, until by 16 hours, the prodissoconch I shell is formed and fully calcified and periostracum is taught over the shell surface. Larvae were reared at 23 ^{o}C and salinity = 34, under atmospheric CO_2.

Figure 5. Calculated response of pH and aragonite saturation state to increasing P_{CO2} from 200 and 1600 μatm (triangles) at typical upwelling conditions along the Oregon coast, for total alkalinity = 2300 μmol kg^{-1}, temperature = 13 ^{o}C, and salinity = 33. Symbols are values of P_{CO2}. Chronic and acute effects due to saturation state decreases from experiments have been noted for bivalve larvae. The Δ 0.3 pH was previously noted as significant to many physiological processes in mollusks (8).

565 Figure 1

566

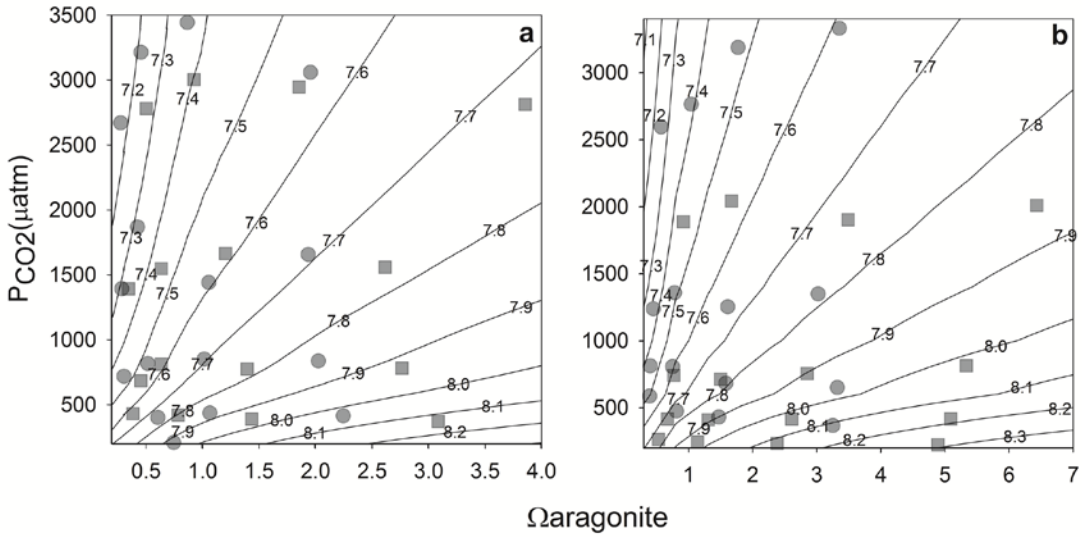

567

568

569

570

571

572 Figure 2

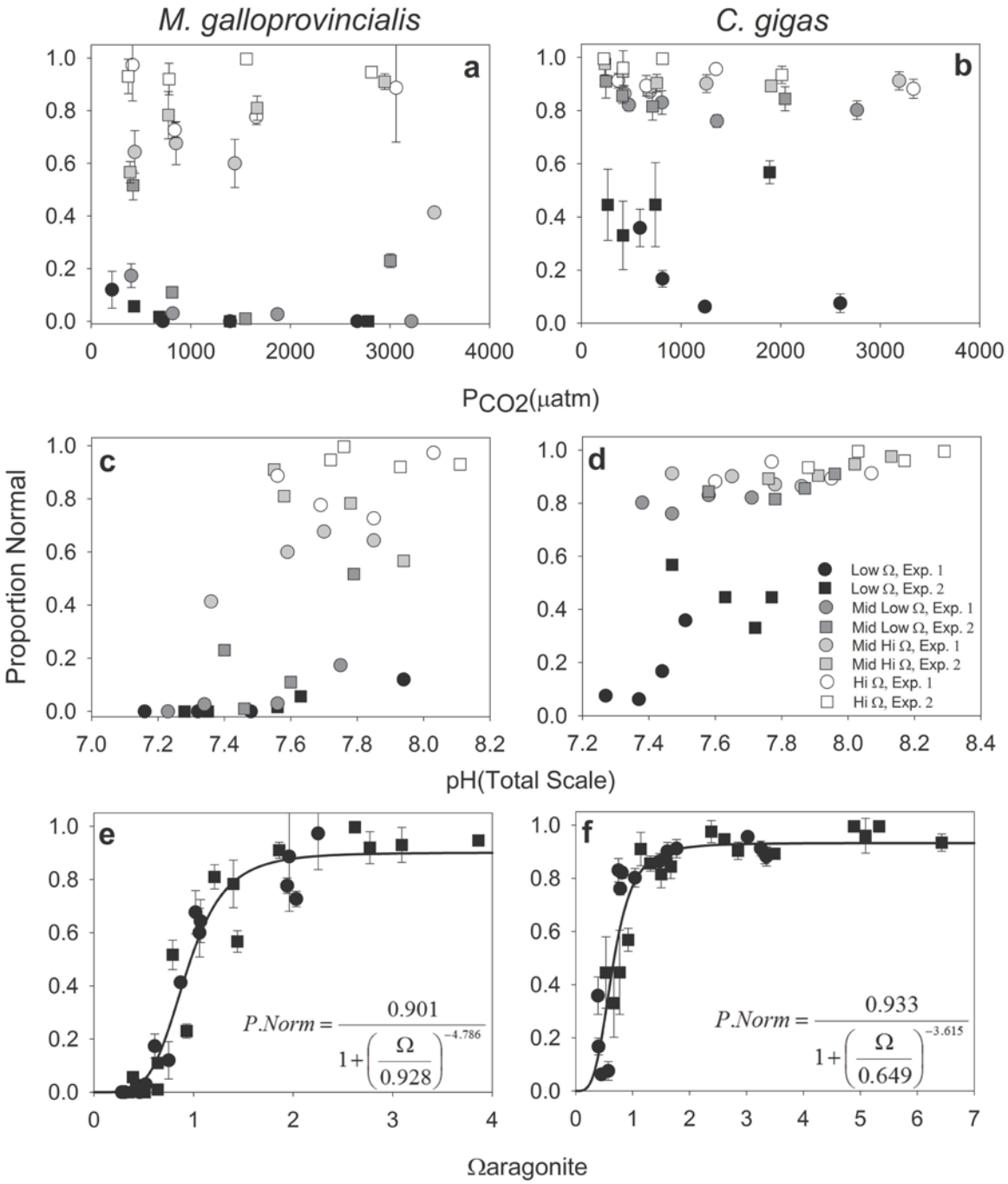

573

574

575

576 Figure 3

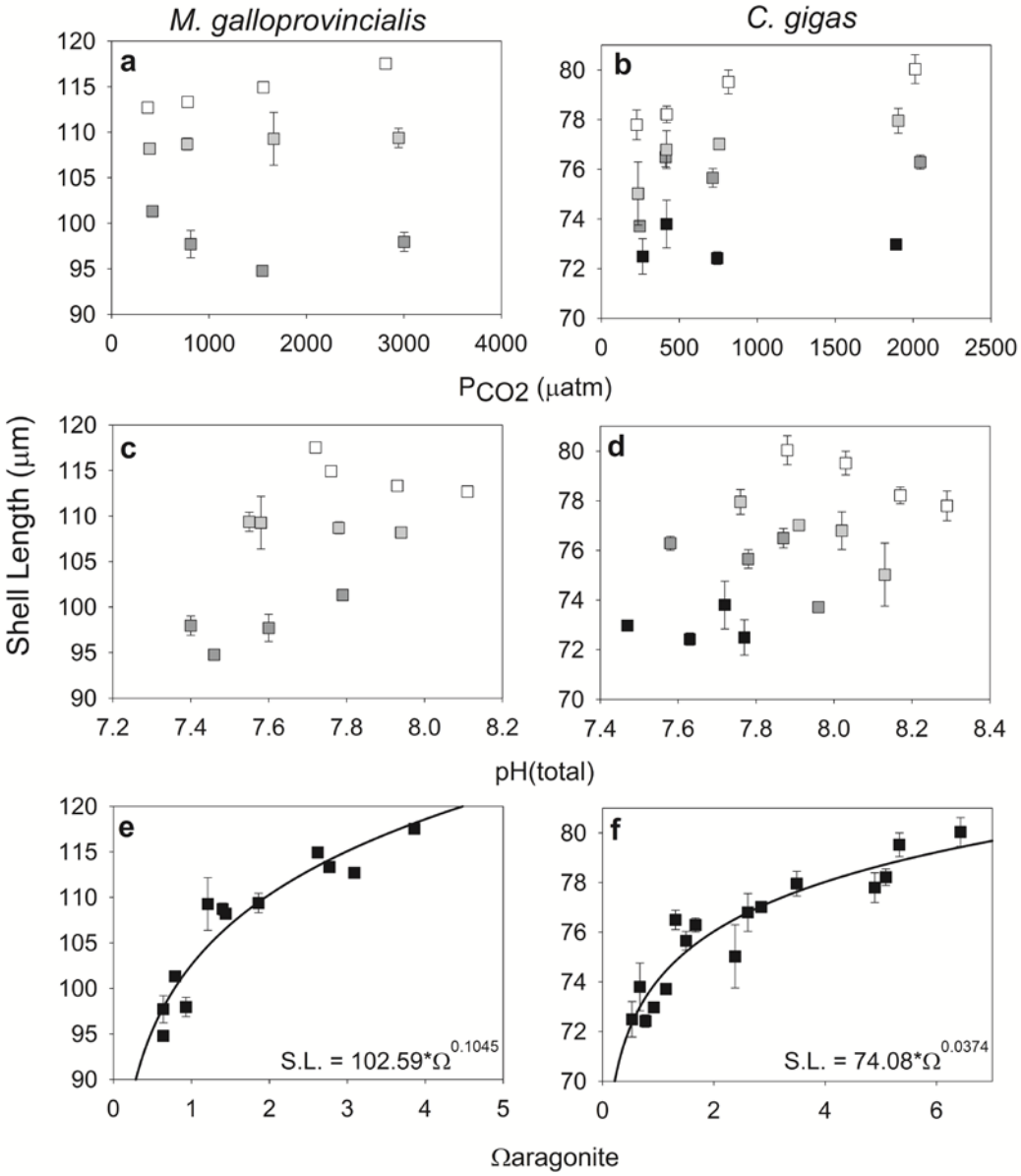

577

578

579

580

581

582

583

584

585

586 Figure 4

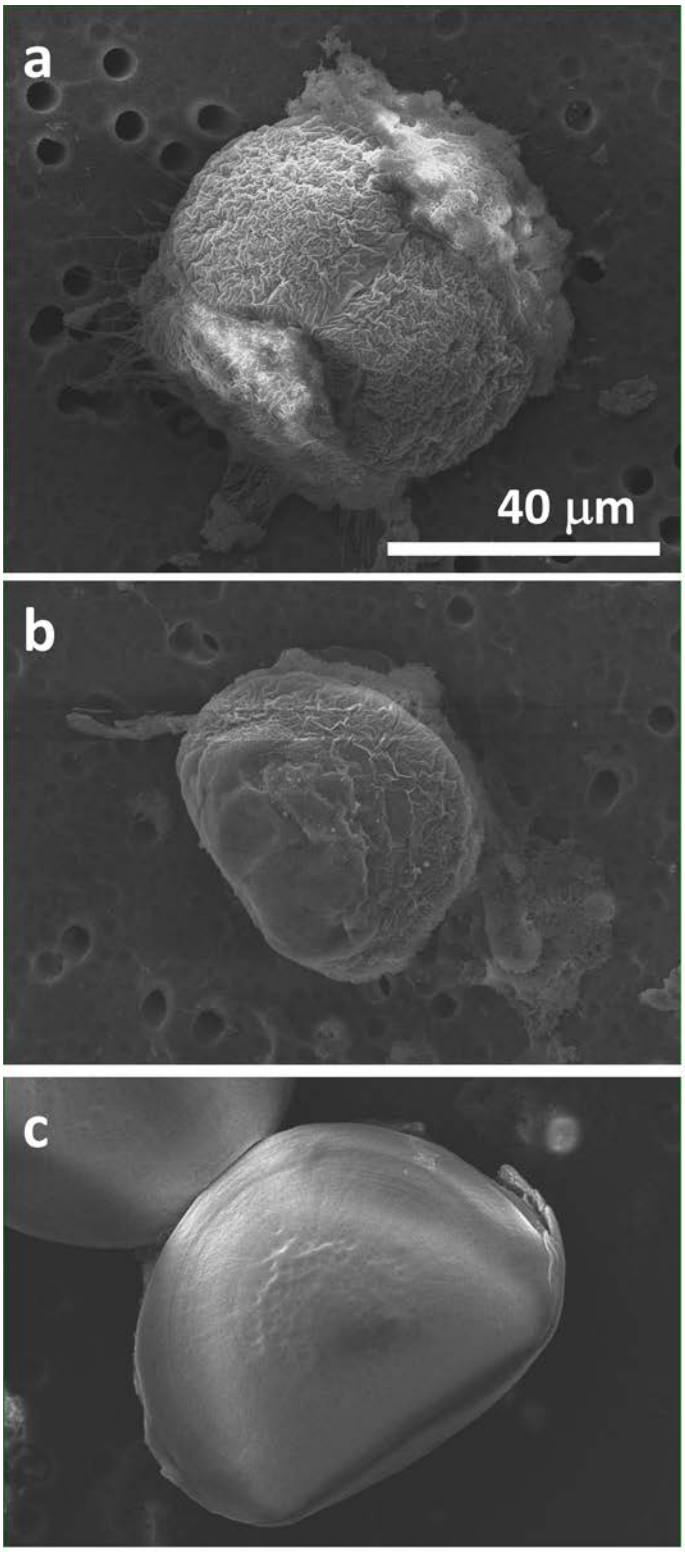

587

588

589 Figure 5

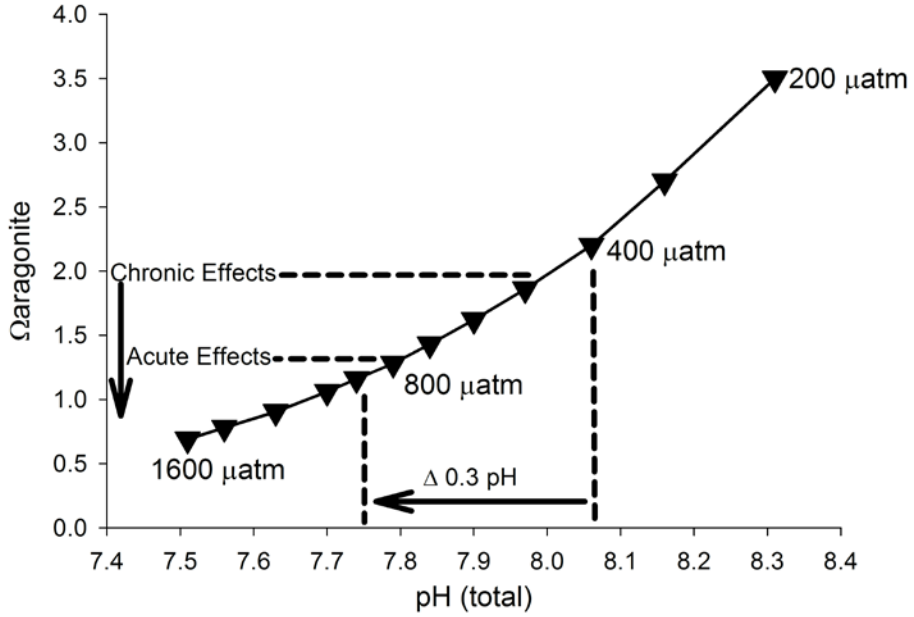

590